

Supramolecular assembly of glucose oxidase on concanavalin A—modified gold electrodes

Diego Pallarola,^{ac} Nuria Queraltó,^b Fernando Battaglini^c and Omar Azzaroni^{*a}

Received 12th January 2010, Accepted 7th April 2010

First published as an Advance Article on the web 7th June 2010

DOI: 10.1039/c000797h

There is a growing quest for the construction of functional supramolecular architectures to efficiently translate (bio)chemical events into easily measurable signals. This interest originates from its inherent scientific relevance as well as from their potential applications in the ever-flourishing areas of bioelectronics and biosensing. Herein, we describe the immobilization of glycoproteins onto electrode surfaces based on recognition-mediated supramolecular processes. Quartz crystal microbalance with dissipation (QCM-D), surface plasmon resonance (SPR) spectroscopy, and electrochemical (EC) measurements were used to characterize the structural and functional features of these bio-supramolecular systems. Carbohydrate–lectin interactions were successfully used to build up stable assemblies of glucose oxidase (GOx) layers mediated by the recognition properties of concanavalin A supramolecular architectures. The catalytic response of GOx indicates that the whole population of enzymes incorporated in the supramolecular architecture is fully active. Even though lectin–carbohydrate interactions are rather weak, the multivalency effects prevailing in the supramolecular assembly confer remarkable stability to the interfacial architecture, thus preventing the release of the enzyme from the surface even with high glucose (ligand) concentrations. This approach represents a simple and straightforward route to locally address functional glycoproteins at interfaces. In this context, we consider that the versatility of a supramolecular assembly using biological interactions could open up new ways of envisioning or to generate new ideas for the future development of highly efficient bioelectronic platforms.

1. Introduction

In the recent years we have seen increasing interest in the integration of biomolecular architectures onto electronic platforms in order to create functional bioelectronic devices.¹ Among the wide variety of biomolecular building blocks enzymes are especially important owing to their excellent functional properties, which include activity, selectivity and specificity.² Hence, the major activities in this field were focused on the development of novel interfacial architectures that could incorporate enzymes and thus transduce biorecognition or biocatalytic processes in the form of amplifiable electronic signals. Further development of bioelectronic enzyme applications requires the construction of protein thin films through immobilization of active proteins onto solid substrates, such as gold.² The biosensor performance is strongly dependent on the characteristics of the interfacial architecture and the quality of the association between the enzyme and the

electrode surface. As a consequence, the enzymes are generally immobilized in artificial microenvironments, subjected to interactions different from those found in their natural environment. Apart from retaining the conformation and biological activity of the biomolecule, the immobilisation procedure must guarantee the accessibility of its active site to the target analyte and other molecules involved in the biorecognition event. Thus, the choice of the bioelectrode construction technique may contemplate a wide range of parameters, including enzyme stability, reproducibility, and kinetic aspects, among others.^{1,2} To achieve this goal different immobilization strategies were developed in recent years. Most of them include adsorption, cross-linking with bifunctional chemical reagents, entrapment in different matrices, electropolymerization, or biotinylated enzymes, just to name a few examples.^{2b} However, it is well known that such methodologies can induce conformational changes in the enzyme, which could be accompanied with a significant loss of enzymatic activity. For example, when biomolecules bind to a substrate through one or two functional groups located on their periphery and not involved in their active site, no significant differences exist in using a random or an oriented immobilization strategy. However, covalent multi-point attachment is more likely to disrupt the folding and functionality of the native biomolecule if essential groups are involved in the binding process.³

Compared with the usually used covalent immobilization or incorporation into sol–gel derived matrix, recognition directed-assembly technique represents an interesting and attractive

^a Instituto de Investigaciones Fisicoquímicas Teóricas y Aplicadas (INIFTA), Departamento de Química, Facultad de Ciencias Exactas, Universidad Nacional de La Plata, CONICET, CC 16 Suc. 4 (1900) La Plata, Argentina.
E-mail: azzaroni@inifta.unlp.edu.ar;

Web: <http://sofmatter.quimica.unlp.edu.ar>

^b Max-Planck-Institut für Polymerforschung, Ackermannweg 10 (55128) Mainz, Germany

^c INQUIMAE—Departamento de Química Inorgánica, Analítica y Química Física, Facultad de Ciencias Exactas y Naturales, Universidad de Buenos Aires, Ciudad Universitaria, Pabellón 2, C1428EHA Buenos Aires, Argentina

alternative due to its simplicity and versatility.⁴ This methodology is also known as “affinity layering” and represents a robust bioaffinity-based immobilization procedure without requiring chemical modification steps.⁴ This is applicable to native proteins and is exclusively based on the different supramolecular interactions that living systems use to form molecular complexes. These non-covalent approaches are based on the remarkable selectivity of the interaction between the constituting building blocks which in turns leads to fast and easy immobilization protocols avoiding the deterioration of the catalytic activity of the enzymes.^{5–7}

Another key advantage of this strategy is that immobilizing a glycoenzyme through its carbohydrate moiety is not likely to affect its prosthetic site. The carbohydrate region is generally located in areas that are not involved in enzyme activity, and therefore it can retain most of their biological function even when their carbohydrate regions are conjugated or blocked.^{4–6} Concanavalin A (Con A) is one of the lectin proteins found in jack bean and exists as a tetramer with a molecular mass of 104 000 Da at a neutral pH.⁸ Each Con A monomer contains one calcium ion binding site, one transition metal binding site, and one carbohydrate binding site (specific to α -D-mannose and α -D-glucose), also referred to as the combining site.⁹ The carbohydrate binding site is near the metal binding sites, but they do not overlap.¹⁰ These properties allow Con A to act as a bioaffinity bridge between a sugar-modified surface and the glycoprotein. This kind of oriented immobilization provides good steric accessibility, as the carbohydrate residues are usually located far away from the active site. Notably, in spite of the widespread use of bioaffinity immobilization in many biochemistry-related fields,^{4–7} little is known about its use in bioelectrochemistry and how its implementation can affect the performance and functionality of enzymatic bioelectrodes.^{11–13} More important, to the best of our knowledge no quantitative study about the bioelectrocatalytic properties of affinity-based enzymatic electrodes has been reported so far.

In this work, we describe the construction of highly efficient mono- and multilayered enzymatic bioelectrodes through recognition-mediated supramolecular processes that closely resemble the well-known bioaffinity immobilization protocols. We have chosen glucose oxidase (GOx) as the model glycoenzyme for two main reasons: (a) its high affinity to Con A and accessible sugar groups for binding, and (b) its wide relevance in diverse technological fields. The results presented here quantitatively reveals that the glycoprotein is efficiently incorporated on the electrode surface and the whole population remains fully active in the biosupramolecular assembly. Furthermore, combined surface plasmon resonance spectroscopy and electrochemical studies corroborated that no leaching-out of the glycoprotein from the electrode takes place at high glucose concentrations.

2. Experimental

Materials

Canavalia ensiformis Concanavalin A (Con A, jack bean), cystamine dihydrochloride (Cys), α -D-mannopyranosylphenyl isothiocyanate (Man), and β -D-glucose were purchased from

Sigma. Glucose oxidase (GOx, *Apergillus niger*) was obtained from Calzyme Laboratories, Inc. The molecular mass of the enzyme (159790 ± 798 Da) was determined by MALDI-TOF-MS analysis following a procedure previously reported.¹⁴ The $[\text{Os}^{\text{II}}(\text{bpy})_2\text{pyCl}]\text{PF}_6$ was synthesized as previously described,¹⁵ where bpy stands for bipyridine and py for pyridine. All other reagents were analytical grade.

Construction of self-assembled layers

The construction of molecular assemblies was prepared using a BK7 glass coated with 2 nm of chromium and 50 nm of gold by evaporation. The substrate was incubated overnight with a 5 mM ethanolic cystamine dihydrochloride solution. Afterwards, the electrode was rinsed with ethanol and dried with N_2 followed by 2 h incubation in a $10 \mu\text{g mL}^{-1}$ α -D-mannopyranosylphenyl isothiocyanate solution in 0.05 M pH 7.4 PBS buffer. Then, the electrode was rinsed with PBS buffer and immersed for 1 h in a $1 \mu\text{M}$ ConA solution in PBS buffer containing CaCl_2 0.5 mM and MnCl_2 0.5 mM.¹⁶ The same buffer was used to incorporate the GOx to the surface and to rinse the electrode after a ConA or GOx assembling step. To immobilize the enzyme on the ConA-modified surface the electrode was incubated for 1 h in a $1 \mu\text{M}$ GOx solution. The modification process was repeated to build up multilayer assemblies. All steps were carried out at room temperature (*ca.* 20 °C).

Surface plasmon resonance (SPR) spectroscopy

SPR detection was carried out in a homemade device using the Kretschmann configuration. The SPR substrates were BK7 glass slides evaporation-coated with 2 nm of chromium and 50 nm of gold. To estimate the Con A or GOx coverage during the sequential assembly steps, the SPR signal at different angles was recorded prior to and after injection of the corresponding protein solution in the liquid cell. This was done to detect the shift of the minimum angle of reflectance due to the protein assembly on the surface. The SPR angle shifts were converted into mass uptakes *via* the experimentally determined relationship, Γ (nanograms per square millimetre) = $\Delta\theta/\text{degrees}/0.19$. The sensitivity factor was obtained by procedures reported in the literature.^{17,18}

Quartz crystal microbalance with dissipation (QCM-D)

The QCM-D measurements were carried out at 21 °C using a Q-Sense microbalance (Q-Sense, Göteborg, Sweden). This instrument allows for a simultaneous measurement of frequency change (Δf) and energy dissipation change (ΔD) by periodically switching off the driving power of the oscillation of the sensor crystal and by recording the decay of the damped oscillation. The time constant of the decay is inversely proportional to D , and the period of the decaying signal gives f . Experiments were performed using commercially available (QSX-301, Q-Sense) gold-coated quartz crystals.

Electrochemical measurements

Cyclic voltammetry experiments were performed with a μ Autolab potentiostat (Echo Chemie) using a three-electrode cell equipped with an Ag/AgCl reference electrode and

platinum mesh counter electrode. All electrochemical experiments were carried out at room temperature (*ca.* 20 °C) in a Teflon cell designed in a way that exposes to solution a 0.18 cm² surface of the electrode. Electrochemical experiments were carried out in a 0.05 M KH₂PO₄/K₂HPO₄, 0.1 M NaCl buffer solution, pH 7.4. In all experiments argon bubbling was used to remove dissolved oxygen from the measurement solutions for at least 30 min before using and for 10 min between successive measurements.

3. Results and discussion

3.1 Recognition-mediated assembly of concanavalin A and glucose oxidase onto gold electrodes

The first step, prior to creating the enzyme glycoassembly, is the immobilization of a Con A monolayer on the electrode surface. Diverse strategies have been reported on the development and optimization of Con A attachment chemistry.¹⁹ Even though the main aim of these approaches has been the creation of affinity-based assemblies, most of them rely on the covalent anchoring of the very first Con A layer.²⁰ Typically, this is performed by reacting surface-bound active groups and peripheral lysine groups in the protein. However, in spite of the robustness of this approach, the multi-site chemical modification of the protein could affect its molecular recognition properties.

On the other hand, the binding of proteins to monovalent carbohydrate moieties is often weak,²¹ yet the presence of multivalent interactions can result in the formation of numerous simultaneous complexation events that proceed to afford high affinity. It is well known that carbohydrates immobilized on a surface are presented multivalently²² and, as such, the lectin binding to a multivalent array is more avid and of higher specificity than the interactions of the monovalent counterparts.^{23,24} This enhanced bioaffinity facilitates the construction of stable Con A monolayer assemblies onto the gold electrodes by simply engineering their surfaces with carbohydrate moieties.^{25–27} To achieve this goal we proceeded to functionalize gold electrodes with mannose groups by following the procedure described by Willner and co-workers.²⁸ Gold surfaces were treated with an ethanolic solution of cystamine. The resulting self-assembled cystamine monolayer-modified electrodes were then modified with isothiocyanatophenyl α -D-mannopyranoside in phosphate buffer (pH = 7.4), to yield the thiourea-monosaccharide monolayer-modified electrodes of phenyl α -D-mannopyranoside (Fig. 1).

Then, we proceeded to the formation of the glycoassemblies on the gold surfaces. This step was monitored by the combined use of quartz crystal microbalance (QCM) and surface plasmon resonance spectroscopy (SPR) techniques. Fig. 2a depicts changes in frequency if a mannosylated gold-coated sensor is in contact with a 1 μ M Con A in PBS buffer solution. The initial exposure to the Con A solution leads to a rapid decrease in frequency followed by slight steady decrease before reaching the final plateau. These frequency changes can be translated into mass coverage in accordance to the Sauerbrey equation:²⁹

$$\Delta m = -\frac{CAf}{n} \quad (1)$$

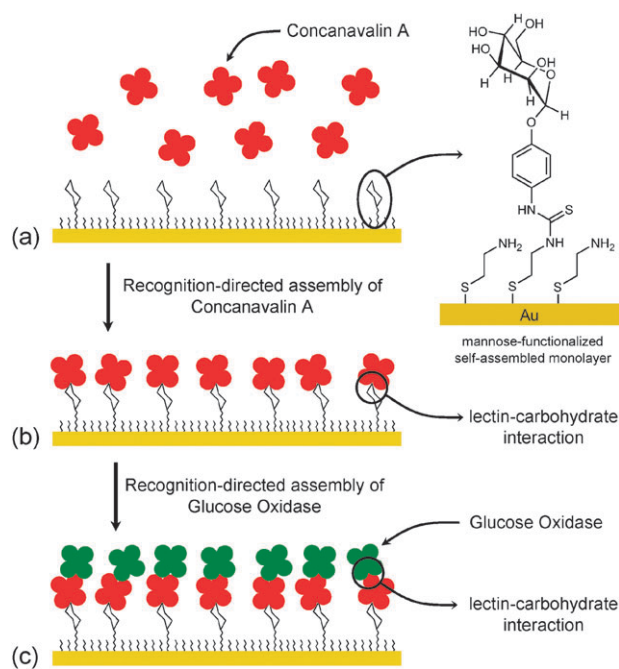


Fig. 1 Scheme describing the recognition-directed assembly of concanavalin A onto the mannosylated gold electrode (a, b) followed by the biosupramolecular immobilization of glucose oxidase onto the Con A-terminated surface (c). Also shown is the chemical structure of the mannose linker coupled to the cystamine self-assembled monolayer.

where n is the overtone number, and C is the mass sensitivity constant. In our experimental setup, C corresponds to 17.7 ng Hz⁻¹ cm⁻², and we have used different overtones for estimating the mass of the immobilized proteins. Accordingly, the mass uptake associated with the rapid f decrease resulted in 253 ng cm⁻². The protein immobilization led to the deposition of 734 ng cm⁻² during the first 60 s of conjugation. Then, the mass steadily increased until reaching a plateau corresponding to 1038 ng cm⁻². On the other hand, the dissipation (ΔD) slowly increased during the conjugation of Con A. The increase in energy dissipation is due to the nonrigid structure of the protein film conjugated on the gold-coated quartz crystal. The D factor is defined as the ratio between the energy dissipated per cycle of oscillation and the total energy stored in the oscillating system, that is, sensor surface + film. During recent years, there has been an increasing effort on understanding and relating dissipative losses (changes in D) to physical processes (interfacial and/or internal friction) occurring at the biomolecular layer. If the immobilized film is rigidly anchored, implying no changes in the coupling between the sensor and liquid environment, no changes of the energy dissipation are detected. On the other hand, D may suffer significant changes if the deposited film is not rigidly attached to the oscillating sensor surface. In other words, a soft film attached to the quartz crystal is deformed during the oscillation, which gives a high dissipation, while as a rigid material it gives a low dissipation.³⁰ In the case of the Con A immobilized on the mannosylated surface, changes in D are reflecting structural changes in the film layer upon immobilization.

In order to precisely define the mass of Con A firmly anchored on the gold-coated crystal³¹ we rinsed the sensor

with buffer after reaching the late stages of the conjugation. Slight but detectable changes in frequency and dissipation during buffer rinsing corroborate the presence of some Con A molecules nonspecifically adsorbed on the bioconjugate. The estimated mass of Con A conjugated on the mannosylated surface was 890 ng cm^{-2} .

Then, the buffer solution was replaced by GOx solution ($1 \mu\text{M}$ in PBS) which was acting as a biorecognizable building block to be assembled on the Con A layer. In close resemblance to that observed in the conjugation of Con A, the recognition-mediated assembly of GOx displayed a sharp decrease in frequency reaching a plateau after 50–60 min. Similarly, dissipation displayed a pronounced increase during the glycoenzyme assembly and remained almost constant during the entire immobilization process. The increase in energy dissipation can be ascribed to the nonrigid layered structure of the Con A-GOx assembly. Rinsing with buffer did not evidence any significant change in frequency and a slight but appreciable decrease in dissipation. This clearly indicates that the GOx layer that the QCM-D senses is firmly conjugated to the Con A and no unbound glycoenzyme is present at the interface. The estimated mass of GOx assembled on the Con A monolayer was 366 ng cm^{-2} . On the other hand, the decreasing D indicates that the film is changing its viscoelastic properties from a soft state to a more rigid one.

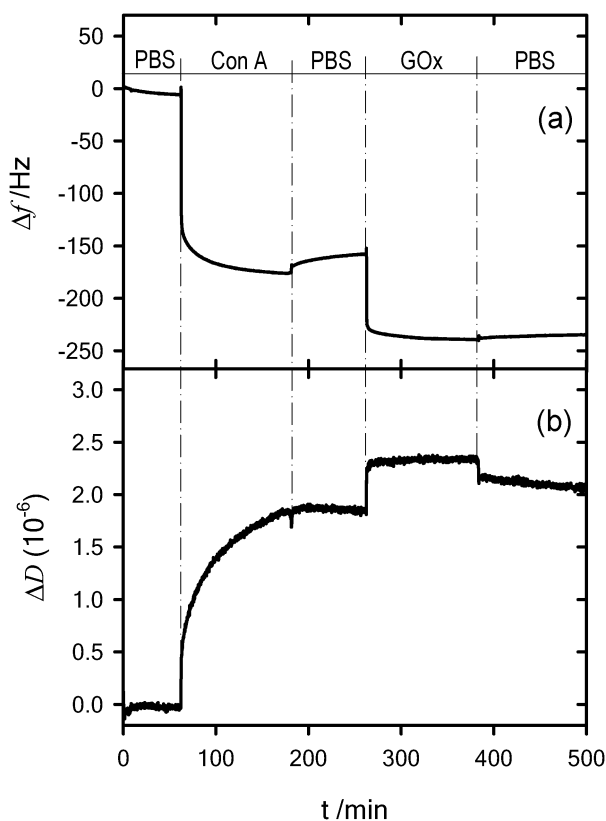


Fig. 2 Quartz crystal microbalance response on (a) frequency and (b) dissipation at the overtone number $n = 3$ (15 MHz) when the concanavalin A–glucose oxidase supramolecular architecture is built-up onto the mannosylated gold-coated quartz crystal through a recognition-directed assembly process.

These changes in dissipation could be attributed to reorganization or conformational changes of the GOx layer resulting in a more compact layer. Similar dissipation behaviour has been recently observed in multilayered supramolecular assemblies.³²

It is worthwhile to mention here that strictly speaking the Sauerbrey equation (eqn (1)) is valid only for uniform rigid films with material properties indistinguishable from those of the crystal resonator. Obviously, this is not the case of soft matter-based architectures attached to the resonator in a liquid environment. Even if the layer is firmly attached, the retained water is not strictly “fixed” to the film. However, in some cases dealing with soft matter the mechanical properties of the film resembles those of a rigid layer in the sense of the Sauerbrey equation. Recently, Notley *et al.* reported that the parameter $\Delta f/n$ in the growth of polyelectrolyte multilayers is independent of frequency throughout the assembly, indicating that the film is rigid enough to use the Sauerbrey equation as a first approximation.³³ In our case, we also observed that during the recognition-driven assembly the normalized parameter $\Delta f/n$ remained independent of the frequency or the overtone number (not shown).

Thereafter, we estimated the mass coverages of Con A and GOx subsequently assembled on the mannosylated gold surface by monitoring the immobilization process using surface plasmon resonance spectroscopy (Fig. 3). Surface plasmon resonance measurements of the mannosylated gold surface prior to and after Con A assembly evidenced a well-defined shift in the minimum of the angular θ -scans of reflected intensity. This $\Delta\theta$ is related to a mass uptake of 185 ng cm^{-2} that corresponds to a surface coverage of $1.8 \times 10^{-12} \text{ mol cm}^{-2}$. This value is in good agreement with spectrophotometric measurements on Con A immobilized on quartz crystal by Anzai *et al.* who estimated $1.6 \times 10^{-12} \text{ mol cm}^{-2}$ for Con A monolayer coverage.³⁴ In a similar vein, the assembly of GOx on the Con A monolayer led to a glycoenzyme mass coverage of 184 ng cm^{-2} , *i.e.*: $1.15 \times 10^{-12} \text{ mol cm}^{-2}$.

The differences in mass uptakes estimated by QCM (Δm_{QCM}) and SPR (Δm_{SPR}) arises from the fact that QCM-D response is extremely sensitive not only to the mass coupled to the quartz crystal surface but also to the viscoelastic properties and density of the film.³⁵ In our case, the film is constituted by Con A molecules conjugated to the mannosylated sensor surface in an aqueous solution. As a consequence, a fraction of solvent is trapped between the adsorbed biomolecules. More important, this retained water is not strictly “fixed” to the film if we consider that it does not behave as the liquid layer above the film. In other words, the QCM detects the solvent that is hydrodynamically coupled to the supramolecular assembly.³⁶ In contrast, the SPR response that originated from refractive index changes as water is replaced by biomolecules, is mostly proportional to the masses of the adsorbed biomolecules. QCM response is not quantitative in the same respect as SPR, since the latter gives a response being proportional to the molecular weight of the adsorbed biomolecules.^{17,37} Hence, the combination of SPR and QCM-D data provides useful information about the structural properties of the adsorbed films, including the water content or “trapped” water by simply taking the difference between Δm_{QCM} and

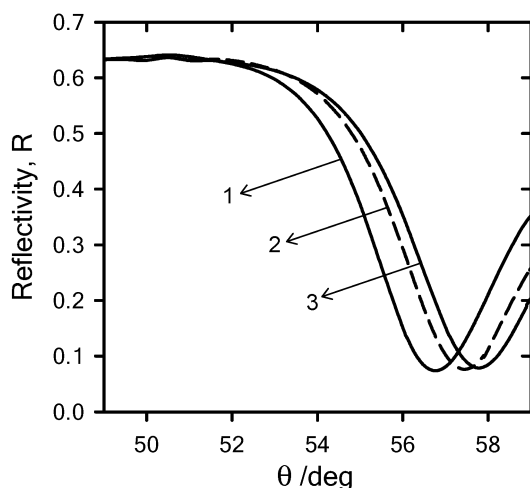


Fig. 3 Reflectivity curves as a function of the angle-of-incidence scan (θ). The plot describes the different reflectivity curves obtained from: (1) mannosylated gold surface, (2) Con A-modified gold surface and (3) GOx-Con A-modified gold surface.

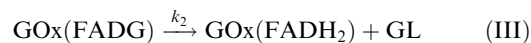
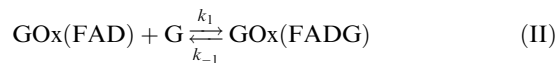
Δm_{SPR} .³⁸ Previous SPR-QCM comparative studies performed on supported phospholipid bilayers, compact streptavidin layers or DNA duplexes indicated that the percentage of water coupled to these films was 25, 55 and 90%, respectively.^{38,39} In our case, 80% of the mass sensed by the QCM-D during the Con A conjugation corresponded to water viscoelastically coupled to the protein film, thus evidencing that the assembly of the lectin led to the formation of water-rich films. In a similar vein, the QCM data of the recognition-mediated assembly of GOx indicated that $\sim 50\%$ of the microgravimetrically sensed mass corresponded to “trapped water”.

3.2 Electrocatalytic activity of GOx monolayers supramolecularly assembled on Con A-modified gold electrodes

Once the glycoenzyme is physically confined on the electrode surface, the oxidoreductase (biocatalytic) reaction is translated into an electrode process *via* the electron transfer mediation of an electron acceptor (donor) of the enzyme in an oxidation (reduction) reaction. The electron acceptor is reduced by the enzymatic reaction, and the reduced form returns to the oxidized form using the electrode as a final electron acceptor. This electron acceptor (donor)-mediated enzyme-electrochemical oxidation (reduction) of a substrate is the basis of the bioelectrocatalysis and one of the fundamental principles of “bioelectronics” with immediate implications in the design and development of biosensors that are now in practical use for measuring blood glucose and for fundamental studies of biofuel cells.⁴⁰

In this context, cyclic voltammetry represents an excellent tool for studying the bioelectrocatalytic properties of the supramolecular assemblies of glucose oxidase formed on the Con A-modified Au electrodes. The working electrode potential is scanned in the anodic direction to generate the oxidized form of the redox mediator, which in turns triggers the catalytic process giving rise to a bioelectrochemical faradaic current.

To be more precise, the (bio)chemical process involved in the redox-assisted GOx-mediated electrochemical oxidation of glucose consists of the following sequence of reactions:⁴¹



R and O are the reduced ($[\text{Os}^{\text{II}}(\text{bpy})_2\text{pyCl}]^+$) and oxidized ($[\text{Os}^{\text{III}}(\text{bpy})_2\text{py}]^{2+}$) forms of the mediator, respectively ($E^{1/2} = 0.24 \text{ V vs. Ag/AgCl}$). At pH 7.4, FADH₂ is the reduced form of the flavin prosthetic group of the GOx whilst FAD corresponds to the oxidized form. FADG is the enzyme-substrate complex, G is the β -D-glucose, and GL is the glucono- δ -lactone. In the cyclic voltammetric measurements the electrolyte solution is solely constituted of $[\text{Os}^{\text{II}}(\text{bpy})_2\text{pyCl}]^+$ and glucose buffered at pH 7.4.

Typical voltammograms evidencing the catalytic activity of GOx monolayers assembled on Con A-modified electrodes are reproduced in Fig. 4.

We will describe the bioelectrochemical process occurring in the supramolecular architecture using the formalism developed by Saveant and co-workers which has previously been used to estimate the rate constants of electrocatalytic processes involving the use of glucose oxidase.^{42–44} A central aspect of the Saveant formalism is the use of the voltammetric response to elucidate the enzymatic activity and, hence, estimate the characteristic rate constants of the catalytic process. These authors derived an expression relating the current increase of the enzyme-catalyzed reaction (j_{cat}) to diverse experimental parameters:

$$\frac{1}{j_{\text{cat}}} = \frac{1}{2F\Gamma_{\text{GOx}}k_3(C_{\text{O}})_0} + \frac{1}{2F\Gamma_{\text{GOx}}} \left(\frac{1}{k_2} + \frac{1}{k_{\text{red}}C_{\text{G}}^0} \right) \quad (2)$$

$(C_{\text{O}})_0$ is the concentration corresponding to O, *i.e.*: $[\text{Os}^{\text{III}}(\text{bpy})_2\text{py}]^{2+}$, at the electrode surface, C_{G}^0 is the glucose concentration, Γ_{GOx} is the total surface concentration of catalytically active enzyme assembled on the electrode and $k_{\text{red}} = k_1k_2/(k_{-1}+k_2)$. j_{cat} can be derived from the experimental data by simply subtracting the voltammetric curve in the absence of glucose to that obtained in its presence.

It becomes clear that at each glucose concentration, a straight line should be obtained upon plotting $1/j_{\text{cat}}$ against $1/(C_{\text{O}})_0$. In the Saveant formalism this representation is denominated “primary plot” and is easily obtained from the voltammetric data in a straightforward manner without requiring a series of experiments varying the mediator concentration in the solution.⁴¹ Primary plots obtained at saturation coverage of GOx assembled on the Con A-modified Au electrode and at several concentrations of glucose are displayed in Fig. 5. It can be clearly seen that they are satisfactorily linear and parallel as predicted from eqn (2). SPR measurements indicated that Γ_{GOx} was $1.15 \times 10^{-12} \text{ mol cm}^{-2}$

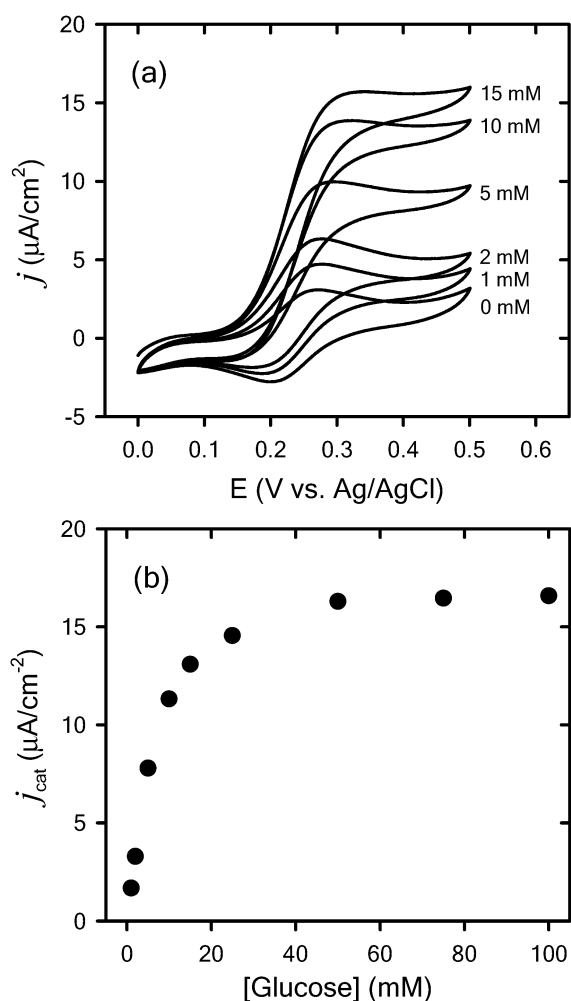


Fig. 4 Cyclic voltammograms describing the bioelectrocatalysis of glucose oxidation occurring at the (Con A)₁(GOx)₁-modified gold electrode prepared by the bioaffinity technique. The experiments were performed using [Os^{II}(bpy)₂pyCl]⁺ (0.1 mM) as mediator in different concentrations of glucose (phosphate buffer, pH 7.4). *T* = 298 K, *v* = 5 mV s⁻¹. (b) Bioelectrocatalytic currents measured on (Con A)₁(GOx)₁ assemblies as a function of substrate concentration. Mediator: 0.1 mM [Os^{II}(bpy)₂pyCl]⁺. *T* = 298 K.

(≡ 184 ng cm⁻²); so, the value of *k*₃ can be estimated directly from the slopes of the linear primary plots. In our experimental scenario the estimated *k*₃ (Os^{II}(bpy)₂pyCl⁺ as co-substrate) corresponded to 8.2 × 10⁵ M⁻¹ s⁻¹. This value is in very good agreement with those reported by Campas i Homs who estimated the electron transfer rate between GOx and different Os(bpy)₂py-related mediators under similar pH conditions.⁴⁵ In these cases, the electron transfer rate constants achieved with osmium mediators having different redox potentials, from 0.175 to 0.65 V (vs. Ag/AgCl), varied from 0.68 × 10⁵ to 1.81 × 10⁶ M⁻¹ s⁻¹. Similar values were previously obtained by Danilowicz *et al.* using Os^{II}(bpy)₂(pyX)Cl⁺ complexes constituted of pyridine derivatives bearing different functional groups (X = COOH, CHO).⁴⁶ Later on, Flexer and co-workers also reported *k*₃ values corresponding to 3.8 × 10⁵ M⁻¹ s⁻¹ for the reoxidation of GOx (FADH₂) in the presence of Os(bpy)₂(py)CHOCl at pH 7.⁴⁷

The “secondary plot” may then be derived by plotting the intercepts of the primary plots against 1/*C*_G⁰. Using eqn (2) *k*_{red} and *k*₂ can be derived from the slope and intercept of the secondary plot, respectively (Fig. 5b). In our case, *k*_{red} and *k*₂ values corresponded to 1.2 × 10⁴ M⁻¹ s⁻¹ and 508 s⁻¹, respectively. It is worthwhile mentioning that all these kinetic constants are in good agreement with those determined in homogeneous solution (see above and Table 1). This fact clearly evidences that the catalytic behaviour of the surface-confined supramolecularly assembled GOx monolayer closely resembles the one that is observed in solution. Or, in other words, we can infer that the GOx monolayer confined on the Au electrode surface *via* a recognition-directed assembly process retains to a great extent its catalytic activity.

3.3 Layer-by-layer concanavalin A-glucose oxidase assemblies on gold electrodes: Nanoconstruction of multilayered bioelectronic interfaces *via* biomolecular recognition

Much of the inspiration to construct interfacial architectures arises from the versatility of noncovalent interactions to

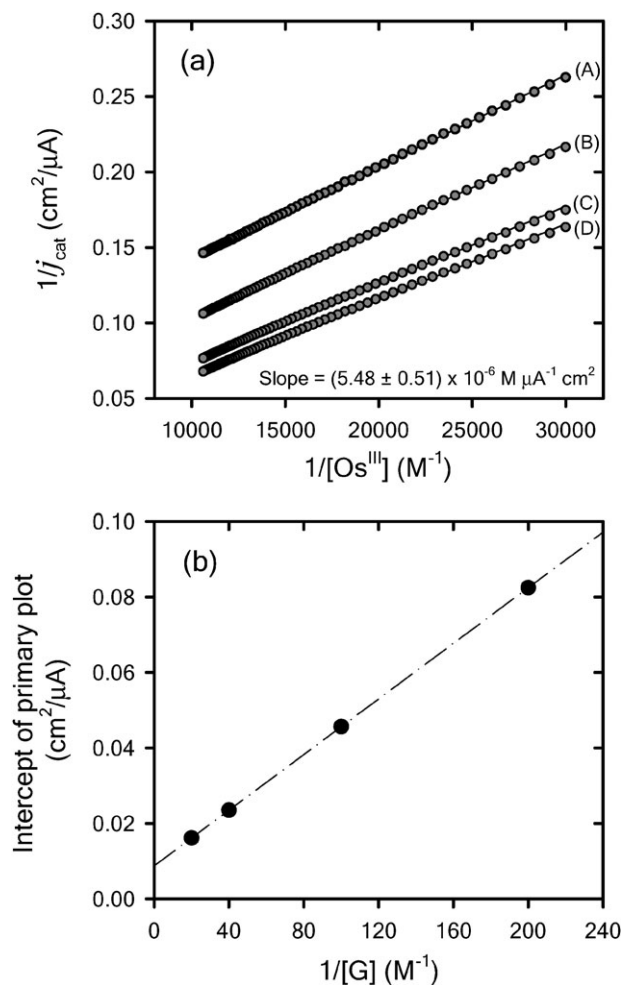


Fig. 5 (Con A)₁(GOx)₁-modified gold electrode. (a) Primary plots obtained for different glucose concentrations: (A) 5 mM (B) 10 mM (C) 25 mM (D) 50 mM. $\Gamma_{\text{GOx}} = 1.15 \text{ pmol cm}^{-2}$. (b) Secondary plot derived from the intercepts of the primary plots in (a). See text for details.

Table 1 Rate constants corresponding to the glucose oxidation reaction catalyzed by glucose oxidase (GOx) molecules supramolecularly immobilized on gold electrodes and in homogeneous solution

Rate constant	Supramolecularly immobilized GOx (this work)	GOx in homogeneous solution (from the literature)
k_3 ($M^{-1} s^{-1}$)	$(8.2 \pm 1.7) \times 10^5$	$(2.2 \pm 0.2) \times 10^{5a}$
k_2 (s^{-1})	508 ± 82	680 ± 100^b
k_{red} ($M^{-1} s^{-1}$)	$(1.2 \pm 0.2) \times 10^4$	$(1.1 \pm 0.2) \times 10^{4b}$

^a Data obtained from ref. 48 using $[Os^{II}(bpy)pyCOOH]^+$ as mediator (pH 7). ^b Data taken from ref. 49 using ferrocene methanol as mediator (pH 8).

assemble diverse functional building blocks.⁵⁰ In particular, specific ligand–receptor interactions have proven very efficient in creating a wide variety of functional assemblies constituted of all-protein thin films.⁵¹ Along these lines, the nanoconstruction of enzyme-containing multilayered thin films resulted particularly attractive owing to the precise control over the loading of the enzyme and the topological characteristics of the multi-enzyme film. For example, biological affinity, such as antibody-antigen and avidin–biotin, has been exploited to build-up multilayered assemblies of antibody-GOx conjugate and *anti*-GOx antibody on electrode surfaces.⁴¹ Similarly, biotin-labeled enzymes and avidin were assembled alternately and repeatedly on the electrode surface to construct multilayer-modified biosensors.^{43,44} In this context, the lectin–sugar system provides another tool for constructing (glyco)enzyme multilayer films and, as qualitatively demonstrated by Anzai and coworkers, also enables the formation of ordered multilayered assemblies constituted of the lectin Con A and the glycoenzyme GOx.⁵² In this section we will describe in quantitative terms the electrocatalytic functional properties of multilayered Con A-GOx assemblies.

To estimate the surface coverage of the proteins incorporated into the interfacial architecture upon the sequential recognition-directed assembly of Con A and GOx, the multilayer growth on the mannosylated gold electrode was characterized by SPR.^{37,53} Fig. 6 shows the different reflectivity curves obtained during the layer-by-layer growth of GOx mediated by the Con A bio-recognition. SPR response originates from refractive index changes as water is replaced by the biomolecules and the shifts in the minimum of the angular scans of reflected intensity ($\Delta\theta$) permits to monitor the sequential assembly of the different biomolecular building blocks onto the interfacial architecture. These reflectivity shifts can also be correlated to mass coverage. In our case, from the corresponding angular variations we estimated the $\Gamma_{Con A}$ and Γ_{GOx} values listed in Table 2.

Once having corroborated the successful multilayered growth of Con A-GOx assemblies we studied their electrocatalytic behaviour in the presence of the enzyme substrate. Their voltammetric response eloquently illustrates the responsiveness of the GOx-containing supramolecular assembly to the presence of the glucose in the surroundings of the electrode surface (Fig. 7a). To better describe the influence of the GOx overlayers on the electrocatalytic activity of the assembly we have plotted the increase of the current density developed through the electrochemical interface upon increasing the number of GOx monolayers supramolecularly assembled on the electrode surface (Fig. 7b). As expected, the glucose sensitivity of the interfacial assemblies is proportional to the amount of immobilized enzyme.

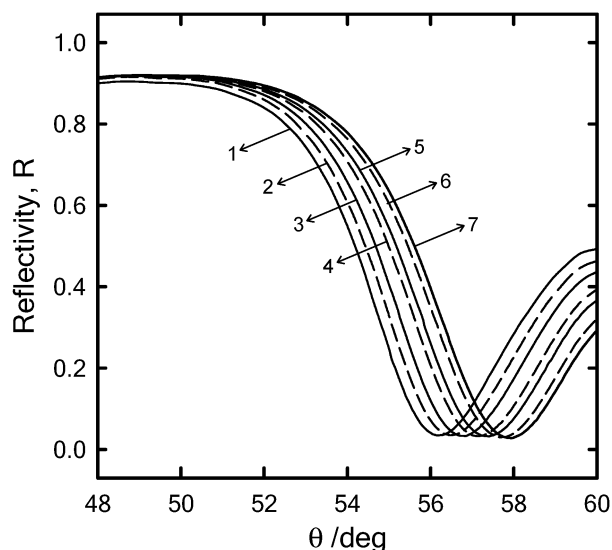


Fig. 6 Reflected intensity as a function of the angle-of-incidence scan (θ) plot describing the supramolecular assembly of the multilayered Con A-GOx structure on the Au electrode. The reflectivity shifts are evidencing the sequential assembly of the different biomolecular building blocks into the interfacial architecture. The different reflectivity curves correspond to: (1) mannosylated Au surface, (2) Con A, (3) (Con A)(GOx), (4) (Con A)₂(GOx), (5) (Con A)₂(GOx)₂, (6) (Con A)₃(GOx)₂, (7) (Con A)₃(GOx)₃.

Furthermore, this experimental result suggests the absence of steric hindrance to the transport of substrate and mediator species into the inner environment of the supramolecular architecture.⁵⁴ As previously described, combined QCM and SPR indicates that the biomolecular assembly contains a large amount solvent, thus reinforcing the idea of a scenario in which glucose and $[Os^{II}(bpy)_2pyCl]^+$ freely diffuse into the all-protein film. So far, we have demonstrated that the first GOx monolayer is fully active and the glucose responsiveness is proportional to the number of GOx monolayers. If we consider the importance of the enzymatic activity in the overall performance of the supramolecular assembly, one key question comes into light: Are the rest of the supramolecularly assembled GOx monolayers fully active as the first one?

To answer this question we represented the bioelectrocatalytic current density as a function of the actual amount of GOx incorporated onto the electrode surface, as determined by SPR. Considering that j_{cat} solely depends on the coverage of the active interacting enzymes and assuming that the interfacial architecture has no influence on the enzyme activity or the transport of substrate or mediator species, we can infer that the bioelectrocatalytic current developed through the

Table 2 Surface coverages of concanavalin A (Con A) and glucose oxidase (GOx) as determined by surface plasmon resonance (SPR) spectroscopy

Assembly (Con A) _n (GOx) _n	$\Gamma_{\text{ConA}}^n \times 10^{12}/\text{mol cm}^{-2}$	$\Gamma_{\text{GOx}}^n \times 10^{12}/\text{mol cm}^{-2}$	$\Gamma_{\text{ConA}}^T \times 10^{12}/\text{mol cm}^{-2}$	$\Gamma_{\text{GOx}}^T \times 10^{12}/\text{mol cm}^{-2}$
$n = 1$	1.88	1.15	1.88	1.15
$n = 2$	1.49	0.91	3.37	2.06
$n = 3$	1.44	0.82	4.81	2.88

Superindexes n and T denotes the protein incorporated in the n layer and the total amount of protein assembled on the electrode surface, respectively.

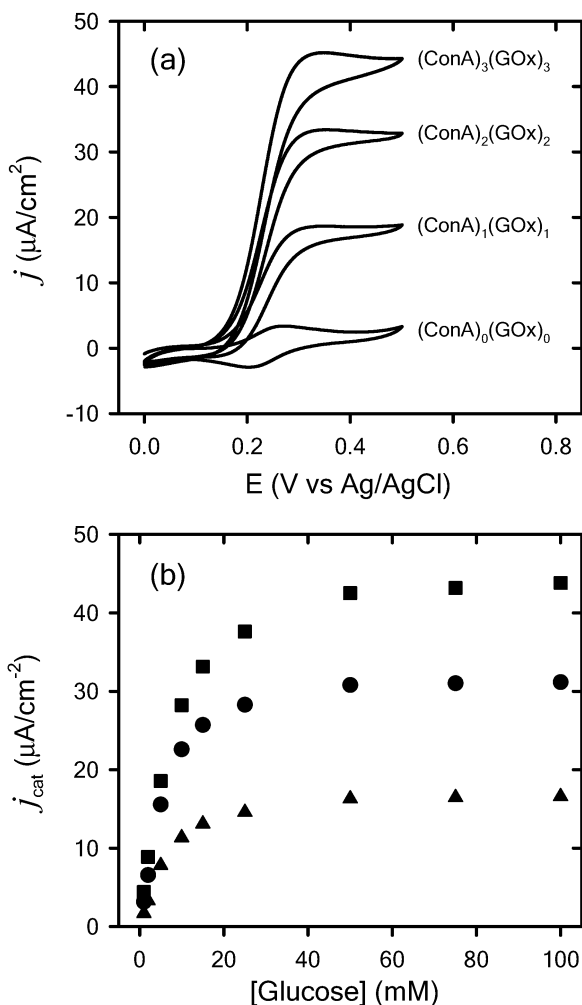


Fig. 7 (a) Voltammetric response of multilayered GOx-modified electrodes prepared by the molecular-recognition assembly technique in the presence of 50 mM glucose, with $[\text{Os}^{\text{II}}(\text{bpy})_2\text{pyCl}]^+$ (0.1 mM) as mediator, in phosphate buffer (pH 7.4). Temperature: 298 K, $\nu = 5 \text{ mV s}^{-1}$. (b) Catalytic response of GOx-containing biosupramolecular electrodes as a function of the number of GOx layers in the presence of increasing amounts of substrate: (▲) (Con A)₁(GOx)₁, (●) (Con A)₂(GOx)₂ and (■) (Con A)₃(GOx)₃. $[\text{Os}^{\text{II}}(\text{bpy})_2\text{pyCl}^+] = 0.1 \text{ mM}$, $\nu = 5 \text{ mV s}^{-1}$, $T = 298 \text{ K}$.

assembly is directly correlated to Γ_{GOx} . Or, in few words, increasing n times Γ_{GOx} will impact on an n -fold increase in bioelectrocatalytic current.

This correlation is illustrated in Fig. 8 together with a linear regression line passing through the origin. The excellent linear behaviour of the correlated experimental values strongly

suggests that, in fact, all the enzyme molecules incorporated in the bioelectrode participate in the electrocatalytic process and are responsible for amplifying the electron transfer across the interfacial architecture.

In the case of these supramolecularly assembled GOx architecture, under substrate saturation conditions, the electrode produced 15.7 μA per picomole of enzyme.

In view of the rapidly growing interest of the scientific community in mastering the formation biosupramolecular assemblies, a non-negligible aspect of these interfacial architectures that deserves further discussion is their stability. One of the remarkable advantages of exploiting carbohydrate–lectin interactions for immobilizing glycoproteins is the intrinsic ability to manipulate and create bioassemblies including hormones, antibodies or enzymes, without affecting their biological activity.^{4–6} In most of cases the carbohydrate region is located in areas that are not involved in the glycoprotein activity and, as such, this methodology could open up new possibilities in supramolecular design. However, it is often claimed that a serious disadvantage of this approach is the typical reversibility of lectin–carbohydrate interactions.^{55,56} Regarding to molecular design of bioelectrode surfaces, the binding reversibility would attempt against the stable anchoring of the glycoprotein⁵⁷ and, as a consequence, biosupramolecular

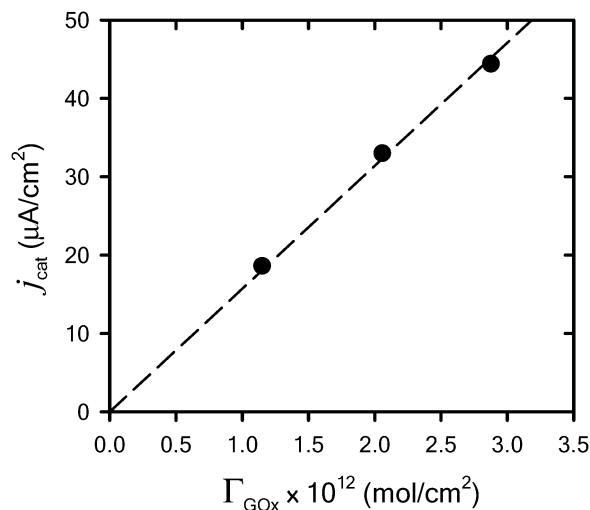


Fig. 8 Representation of the bioelectrocatalytic current density (j_{cat}) as a function of the total amount of glucose oxidase supramolecularly assembled on the electrode surface (Γ_{GOx}), as determined by surface plasmon resonance spectroscopy. The dashed trace corresponds to the regression line. The linear regression model was forced to pass through the origin by setting the intercept parameter to zero and estimating only the slope parameter: $15.7 \mu\text{A pmol}^{-1}$.

enzyme electrodes would not remain stable over time. In fact, extensive work by Anzai and co-workers has demonstrated that the structural stability of sugar–lectin assemblies constituted of glycogen and Con A can be strongly affected by the presence of free ligand in solution, *i.e.*: mannose or glucose.⁵⁸

It is commonly argued that monosaccharide–lectin interactions are relatively weak (in the millimolar range), and may show relaxed or broad recognition specificity because they generally bind to a group of related saccharide structures.⁵⁹ For example, concanavalin A affinity to methyl α -D-mannopyranoside is only 4-fold-higher than to α -D-glucopyranoside.²¹ In our case, we are dealing with supramolecular assemblies constituted of GOx and Con A held together by lectin–carbohydrate interactions in which the enzyme substrate, *i.e.*: glucose, could operate as a specific ligand to Con A. At first sight, this fact would imply that the bioassembly is intrinsically unstable or spontaneously dismantled in the presence of glucose. In principle, cyclic voltammetry results discussed above suggest that the interfacial architecture is stable during the electrochemical runs; however, with the aim of corroborating the stability of the bioassembly, we monitored the protein coverage after placing the (Con A)₃(GOx)₃-modified electrode surface in contact with glucose solution. Fig. 9 displays the SPR sensorgram describing the incubation experiment corresponding to the (Con A)₃(GOx)₃ assembly in 0.1 M glucose (in PBS buffer, pH 7.4). If the reflected intensity at a fixed angle of observation is monitored as a function of time, kinetic information about any changes of the interfacial architecture induced by the presence of glucose could be monitored and analyzed. Even though, it is worthwhile indicating that the reflectivity increase sensed after replacing the buffer by the concentrated glucose solution should be attributed to sharp changes in the optical properties of the liquid medium⁶⁰ and not to surface processes occurring on the electrode interface. The kinetic scan reveals that after incubating the (Con A)₃(GOx)₃ assembly for a period of 30 min in a concentrated ligand solution and thoroughly rinsing the liquid cell with buffer, only slight reflectivity changes are detected. Moreover, the stable baseline obtained in buffer after rinsing the assembly clearly corroborates the robust immobilization of the interfacial architecture *via* lectin–carbohydrate interactions. To quantify these minor changes we compared the recorded angular scans of the (Con A)₃(GOx)₃-modified surfaces prior to and after the incubation in 0.1 M glucose. Considering that the total mass coverage of the Con A-GOx conjugated on the electrode is 960 ng cm⁻², from the reflectivity changes of the (Con A)₃(GOx)₃-Au/electrolyte buffer interface we can conclude that only a negligible fraction of the all-protein film (~ 20 ng cm⁻²) is removed from the assembly due to the presence of free ligand in solution. Furthermore, assuming that the protein loss is exclusively due to the removal of GOx from the outer layer, the shifts in the minimum of the angular scans of reflected intensity would indicate that Γ_{GOx}^T varied from 2.88×10^{-12} to 2.75×10^{-12} mol cm⁻², *i.e.*: 5% decrease, due to the interaction with glucose in solution. In close resemblance, electrochemical experiments on (Con A)₃(GOx)₃ assemblies performed under similar incubation conditions (Fig. 10) also revealed a slight decrease in the catalytic currents from 43.9 to 43.1 $\mu\text{A cm}^{-2}$, *i.e.*: 2%

decrease. This experimental information supports the asseveration that the Con A-GOx interfacial architecture remains stable even in the presence of competitive ligand binding. More important, the competitive binding with free ligands in solution should not be solely ascribed to the interaction with the outer protein layers; electrocatalytic measurements confirmed that glucose is freely interacting with the glycoenzyme along the entire protein film.

If we consider that the construction of our interfacial assembly is mediated by the recognition properties of Con A,⁶¹ which is widely recognized to exhibit weak affinity and broad specificity for the individual ligands, then the remaining question is: Why do we observe remarkable film stability in the presence of concentrated ligand solutions? To address this question we need to refer to the prevailing multivalent interactions that govern the stability of the molecular assembly. Biology has furnished many interesting examples of proteins self-assembling into superstructures wherein the complexes gain or enhance functions with respect to those of the individual components.⁶² Multivalent interactions are especially prevalent in glycobiology⁶³ where high specificity and high

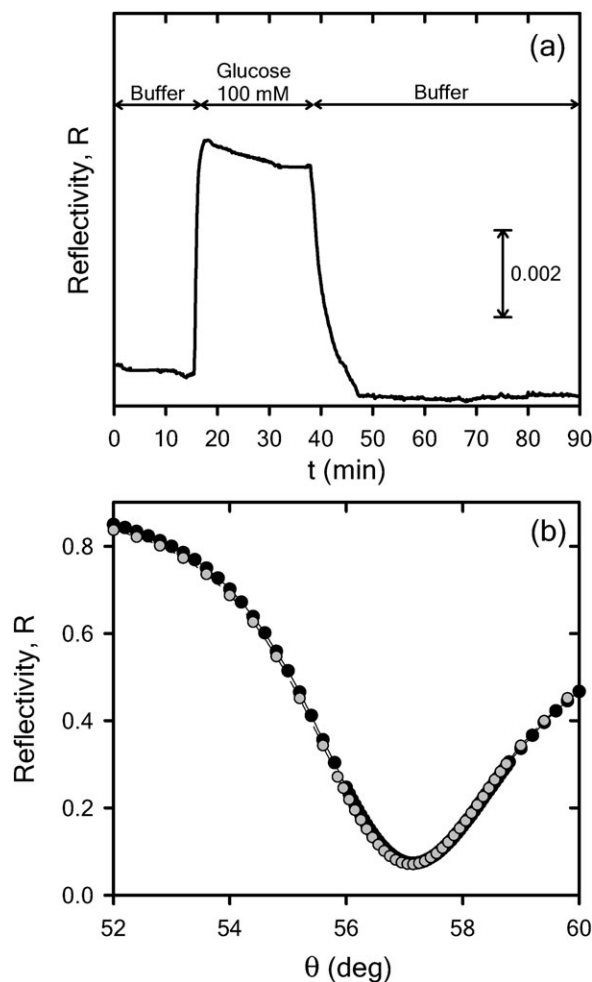


Fig. 9 (a) SPR kinetics describing the incubation of a (Con A)₃(GOx)₃-modified electrode in 0.1 M glucose followed by extensive rinsing with phosphate buffer (50 mM, pH 7.4). (b) Angular reflectivity scans corresponding to the (Con A)₃(GOx)₃-modified electrode prior to (●) and after (○) incubation in 100 mM glucose. In both cases the angular scans were taken in phosphate buffer solution.

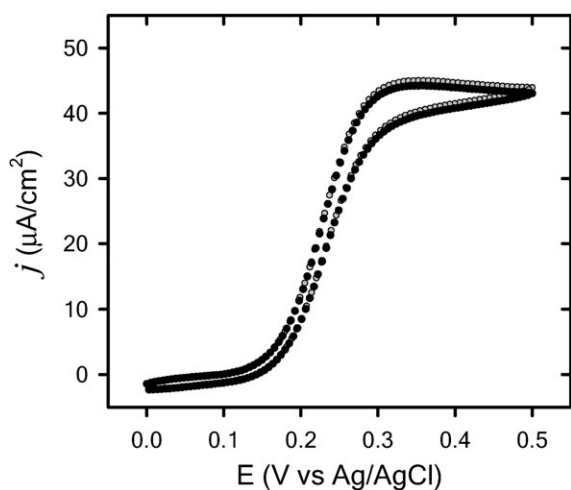


Fig. 10 Cyclic voltammograms describing the bioelectrocatalytic activity of (Con A)₃(GOx)₃-modified Au electrodes in the presence of 100 mM glucose (substrate) + 0.1 mM Os^{II}(bpy)₂pyCl⁺ (mediator). The different traces correspond to the voltammetric responses measured prior to (●) and after (●) incubation in 100 mM glucose during 30 min. $\nu = 5 \text{ mV s}^{-1}$. $T = 298 \text{ K}$.

avidity interactions take place between multimeric lectins and their carbohydrate ligands. More important, this phenomenon occurs in spite of typical low affinity provided by the well-known monovalent carbohydrate–lectin interaction.⁶⁴ Multivalency is a recurrent strategy exploited by microorganisms to remain attached to host cells. For example, *Escherichia coli* use the FimH adhesin located on the tips of its type 1 pili to bind to mannose groups present on the surface of bladder epithelial cells.⁶⁵ Repeated units of ligands and receptors located on opposing surfaces can act cooperatively to enhance their functional affinity and specificity. It has been demonstrated that this can be achieved through ligand multivalency, extended binding regions capable of interaction with more than one single ligand, or clustering of several identical binding sites by formation of protein assemblies. An illustrative example of multivalent enhancement is the case of synthetic polymers carrying multiple mannose residues which exhibited 10⁵-fold higher affinity for Con A than methyl α -mannoside.⁶⁶ On the other hand, ligand multivalency also affects the specificity of lectin–carbohydrate interactions. Kiessling *et al.* reported that whereas concanavalin A binds methyl α -mannose with a 4-fold higher affinity than methyl α -glucose, it discriminates between polyvalent analogues to the corresponding monosaccharides with an up to 160-difference in affinity.⁶⁶

In our case, the sequential protein immobilization is reversing the affinity character of the exposed surface. In close analogy to polyelectrolyte multilayers,⁶⁷ where each polyion is responsible for the reversal of the surface charge, the multivalent character of the biomolecular building blocks is responsible for reversing the ligand–receptor characteristics of the electrode surface. Con A-terminated films exhibit carbohydrate-binding properties, whilst GOx-terminated surfaces display lectin-binding characteristics, thus mimicking the presentation of carbohydrates on the cell surface.⁶⁴ In both cases, the biorecognizable proteins (Con A or GOx) assembling from solution interact with surface-confined clusters of their ligand–receptor counterparts.

This important aspect determines not only the multivalent character of the interfacial assembly but their strong and specific bioaffinity interactions that hold the biosupramolecular architecture together in the presence of concentrated glucose solutions. The critical role of surface ligand clustering on the specificity of lectins was demonstrated by Kahne and co-workers in a series of experiments using a solid-phase carbohydrate library.⁶⁸ The library, which contained approximately 1300 related di- and trisaccharides attached to beads, so that each bead contained clusters of a single carbohydrate species, was screened against *Bauhinia purpurea* lectin. These authors found two ligands that bind more tightly to the lectin than N-acetyllactosamine (the known ligand). Noteworthy, in solution, these derivatives showed no higher affinity to the lectin than N-acetyllactosamine.⁶⁸ Therefore, the amplified affinity and specificity of the lectin to the beads containing the two derivatives appear to result from their polyvalent presentation on the bead surface. Hence, referring back to the Con A-GOx architectures, we can infer that the formation of biorecognizable protein assemblies that act as “ligand clusters” on the electrode surface introduce multivalency effects that confer additional stability to the system. As such, even though carbohydrate–lectin interactions are weak, the presence of multivalent interactions explains the robustness of the biosupramolecular assembly in the presence of free ligand in solution.

Conclusions

In this work, we have described a strategy to build-up functional biomolecular platforms suitable for creating bioelectronic interfacial architectures. This approach was based on the use of concanavalin A as a building block for addressing the immobilization of glucose oxidase *via* a recognition-directed supramolecular assembly process. These biomolecular entities were assembled onto mannosylated gold electrodes through carbohydrate–lectin biological interactions. Combined SPR and QCM studies indicated that the protein assembly leads to the formation of solvent-rich films, in which 80% of the mass sensed by QCM-D corresponded to water viscoelastically coupled to the surface-confined protein conjugate. These Con A-GOx architectures were successfully used for mediating the oxidation of glucose in the presence of a reversible one-electron redox couple, [Os^{II}(bpy)₂pyCl]⁺. By using the Saveant formalism, cyclic voltammetry and SPR-derived information enabled the detailed kinetic characterization of the GOx-containing assemblies. These studies revealed that the dynamics of their catalytic activity toward glucose oxidation is comparable to that reported for experiments performed in solution. This indicates that, even though the interfacial assembly resembles a complex supramolecular system, the electron transfer between the electrode and the prosthetic groups of the enzymatic system by means of [Os^{II}(bpy)₂pyCl]⁺ is not hindered and the recognition-directed immobilization process enables the formation of a fully active GOx monolayer.

Then, the method was extended to the alternate step-by-step assembly of Con A and GOx monolayers onto the mannosylated gold electrode. The lectin was used as a linker to hold together two successive glycoenzyme monolayers *via* carbohydrate–lectin interactions, leading to the formation of

the self-assembling molecular constructions using the specific interaction of the glycosyl groups with Con A. These supramolecular GOx-containing structures gave rise, in the presence of glucose and $[\text{Os}^{\text{II}}(\text{bpy})_2\text{pyCl}]^+$, to large catalytic plateau currents, as determined by cyclic voltammetry. The systematic analysis of these data as a function of SPR-derived GOx coverage demonstrated that the recognition-directed construction of the protein assembly preserves the activity of the enzymatic building blocks and the whole population of GOx incorporated within the assembly participates in the glucose oxidation leading to the bioelectronic readout. This means that the complexity of the supramolecular assembly does not affect the $[\text{Os}^{\text{II}}(\text{bpy})_2\text{pyCl}]^+$ -mediated connectivity and access of substrate and co-substrate to the prosthetic groups of GOx in the bioconjugate layer. The same can be said to for the access to the metal surface, *i.e.*: the interfacial architecture has no influence on the enzyme activity and the transport of substrate or mediator species. Finally, we have demonstrated that relatively weak biological interactions between the constituting building blocks also provide a pathway to create stable supramolecular enzyme electrodes. In this case, the biorecognizable Con A- or GOx-terminated assemblies can act as “ligand clusters” on the electrode surface and, as a result, marked multivalency effects promote an enhancement of the affinity and specificity of the Con A-glycoenzyme interactions. As such, even though carbohydrate-lectin interactions are weak, the presence of multivalency effects explains the robustness of the biosupramolecular assembly in the presence of concentrated glucose (ligand) solutions.

These results using bio-supramolecular architectures demonstrate the potential of spontaneous recognition-driven assembly as a facile strategy to create highly functional interfaces in which the inherent biological features of the building blocks remain unaltered. This approach would enable to locally address bioactive functional units within the supramolecular assembly with molecular precision, representing a crucial feature for the molecular design of biosensing platforms. We consider that this strategy exploiting weak noncovalent interactions in self-organizing biosystems could provide new tools for the facile design of 3D interfacial nanoarchitectures achieving directional electron transport or translating specific chemical events into measurable electronic signals.

Acknowledgements

The authors acknowledge financial support from Max-Planck-Gesellschaft (MPG), Consejo Nacional de Investigaciones Científicas y Técnicas (CONICET) (PIP 2009-0362) Agencia Nacional de Promoción Científica y Tecnológica (BID PICT 00575 y PAE 2006 37063 – PRH 2007 No. 74 – PIDRI No. 74), Centro Interdisciplinario de Nanociencia y Nanotecnología (CINN – ANPCyT) and Alexander von Humboldt Stiftung (Germany). D.P acknowledges CONICET for a postdoctoral fellowship. F.B. and O.A. are CONICET fellows.

References

- (a) I. Willner and E. Katz, in *Bioelectronics: From Theory to Applications*, ed. I. Willner and E. Katz, Wiley-VCH, Weinheim, 2005, ch. 1, pp. 1–13; (b) F. W. Scheller and U. Wollenberger, in *Bioelectrochemistry*, ed. G. S. Wilson, Wiley-VCH, Weinheim, 2002, ch. 13, pp. 431–459; (c) A. Heller and Y. Degani, in *Redox Chemistry and Interfacial Behaviour of Biological Molecules*, ed. G. Dryhurst and K. Niki, Plenum Press, New York, 1988, ch. 11, pp. 151–171; (d) I. Katakis and A. Heller, in *Frontiers in Biosensors I: Fundamental Aspects*, ed. F. W. Scheller, F. Schubert and J. Fedrowitz, Birkhäuser Verlag, Basel, 1997, pp. 220–241; (e) J. Hodak, R. Etchenique, E. J. Calvo, K. Singhal and P. N. Bartlett, *Langmuir*, 1997, **13**, 2708–2716; (f) E. J. Calvo, R. Etchenique, L. Pietrasanta, A. Wolosiuk and C. Danilowicz, *Anal. Chem.*, 2001, **73**, 1161–1168; (g) M. Zayats, B. Willner and I. Willner, *Electroanalysis*, 2008, **20**, 583–601; (h) B. Willner, E. Katz and I. Willner, *Curr. Opin. Biotechnol.*, 2006, **17**, 589–596; (i) Heller and B. Feldman, *Chem. Rev.*, 2008, **108**, 2482–2505; (j) N. Mano, J. E. Yoo, J. Tarver, Y.-L. Loo and A. Heller, *J. Am. Chem. Soc.*, 2007, **129**, 7006–7007; (k) A. Heller, *AIChE J.*, 2005, **51**, 1054–1066.
- (a) B. Willner and I. Willner, in *Bioelectronics: From Theory to Applications*, ed. I. Willner and E. Katz, Wiley-VCH, Weinheim, 2005, ch. 3, pp. 35–97; (b) F. W. Scheller, F. Lisdat and U. Wollenberger, in *Bioelectronics: From Theory to Applications*, ed. I. Willner and E. Katz, Wiley-VCH, Weinheim, 2005, ch. 4, pp. 99–126; (c) T. Ikeda, in *Frontiers in Biosensors I: Fundamental Aspects*, ed. F. W. Scheller, F. Schubert and J. Fedrowitz, Birkhäuser Verlag, Basel, 1997, pp. 243–266; (d) M. Senda and T. Ikeda, in *Macromolecular Complexes: Dynamic Interactions and Electronic Processes*, ed. E. Tsuchida, VCH-Wiley, Weinheim, 1991, ch. 11, pp. 229–249; (e) P. N. Bartlett and C. S. Toh, in *Biosensors: A Practical Approach*, ed. J. Cooper and T. Cass, Oxford University Press, Oxford, 2004, ch. 4, pp. 59–96; (f) F. W. Scheller, C. Bauer, A. Makower, U. Wollenberger, A. Warsinke and F. F. Bier, in *Biomolecular Sensors*, E. Gizeli and C. R. Lowe, Taylor & Francis, London, 2002, ch. 8, pp. 207–238; (g) F. W. Scheller, F. Lisdat, C. Lei, B. Ge and U. Wollenberger, in *Coupling of Biological and Electronic Systems*, ed. K.-H. Hoffmann, Springer Verlag, Heidelberg, 2002, ch. 8, pp. 95–105.
- (a) A. G. Mayes, in *Biomolecular Sensors*, ed. E. Gizeli and C. R. Lowe, Taylor & Francis, London, 2002, ch. 4, pp. 49–86; (b) W. H. Scouten, J. H. T. Luong and R. S. Brown, *TIBTECH*, 1995, **13**, 178–185; (c) B. Prieto-Simón, M. Campàs and J.-L. Marty, *Protein Pept. Lett.*, 2008, **15**, 757–763.
- (a) M. Saleemuddin and Q. Husain, *Enzyme Microb. Technol.*, 1991, **13**, 290–295; (b) M. Farooqi, P. Sosniza, M. Saleemuddin, R. Ulber and T. Scheper, *Appl. Microbiol. Biotechnol.*, 1999, **52**, 373–379; (c) M. Farooqi, M. Saleemuddin, R. Ulber, P. Sosniza and T. Scheper, *J. Biotechnol.*, 1997, **55**, 171–179; (d) S. Husain, F. Jafri and M. Saleemuddin, *Biochem. Mol. Biol. Int.*, 1996, **40**, 1–11.
- (a) J. Turkova, M. Fusek, J. J. Maksimov and Y. B. Alakhov, *J. Chromatogr., B: Biomed. Sci. Appl.*, 1986, **376**, 315–321; (b) H. Rosenfeld, J. Anilyte, H. Helmholz, J. Liesiene, P. Thiesen, B. Niemeyer and A. Prange, *J. Chromatogr., A*, 2005, **1092**, 76–88; (c) F. Santori and J. Hubble, *J. Chromatogr., A*, 2003, **1003**, 123–126.
- (a) H. Yavuz, S. Akgo, Y. Arica and A. Denizli, *Macromol. Biosci.*, 2004, **4**, 674–679; (b) M. V. Miranda, M. L. Magri, A. A. N. del Cañizo and O. Cascone, *Process Biochem.*, 2002, **38**, 537–543.
- Z. Wen and B. Niemeyer, *J. Chromatogr., B: Anal. Technol. Biomed. Life Sci.*, 2007, **857**, 149–157.
- (a) A. Deacon, T. Gleichmann, A. J. Kalb, H. Price, J. Raftery, G. Bradbrook, J. Yariv and J. R. Helliwell, *J. Chem. Soc., Faraday Trans.*, 1997, **93**, 4305–4312; (b) G. M. Edelman, B. A. Cunningham, G. N. Reeke Jr., J. W. Becker, M. J. Waxdal and J. L. Wang, *Proc. Natl. Acad. Sci. U. S. A.*, 1972, **69**, 2580–2584; (c) J. L. R. Arrondo, N. M. Young and H. H. Mantsch, *Biochim. Biophys. Acta, Protein Struct. Mol. Enzymol.*, 1988, **952**, 261–268; (d) G. M. Alter, E. R. Pandolfino, D. J. Christie and J. A. Magnuson, *Biochemistry*, 1977, **16**, 4034–4038.
- (a) J. W. Becker, G. N. Reeke Jr., B. A. Cunningham and G. M. Edelman, *Nature*, 1976, **259**, 406–409; (b) A. J. Kalb and A. Levitzki, *Biochem. J.*, 1968, **109**, 669–672.
- (a) Z. Derewenda, J. Yariv, J. R. Helliwell, A. J. Kalb, E. J. Dodson, M. Z. Papiz, T. Wan and J. Campbell,

- EMBO Journal*, 1989, **8**, 2189–2193; (b) G. N. Reeke Jr., J. W. Becker and G. M. Edelman, *J. Biol. Chem.*, 1975, **250**, 1525–1547.
- 11 (a) Z. Dai, A.-N. Kawde, Y. Xiang, J. T. La Belle, J. Gerlach, V. P. Bhavanandan, L. Joshi and J. Wang, *J. Am. Chem. Soc.*, 2006, **128**, 10018–10019; (b) L. Ding, W. Cheng, X. Wang, S. Ding and H. Ju, *J. Am. Chem. Soc.*, 2008, **130**, 7224–7225; (c) Z. Chen, F. Xi, S. Yang, Q. Wu and X. Lin, *Sens. Actuators B*, 2008, **130**, 900–907; (d) B. Bucur, A. F. Danet and J.-L. Marty, *Biosens. Bioelectron.*, 2004, **20**, 217–225.
 - 12 (a) Y. Kobayashi and J.-i. Anzai, *J. Electroanal. Chem.*, 2001, **507**, 250–255; (b) L. Tan, Q. Xie and S. Yao, *Bioelectrochemistry*, 2007, **70**, 348–355; (c) T. Hoshi, S. Akase and J.-i. Anzai, *Langmuir*, 2002, **18**, 7024–7028.
 - 13 (a) Y. Kobayashi, T. Hoshi and J.-i. Anzai, *Chem. Pharm. Bull.*, 2001, **49**, 755–757; (b) Z. Shen, M. Huang, C. Xiao, Y. Zhang, X. Zeng and P. G. Wang, *Anal. Chem.*, 2007, **79**, 2312–2319; (c) K. Sugawara, T. Shirotori, G. Hirabayashi, H. Kuramitz and S. Tanaka, *J. Electroanal. Chem.*, 2004, **568**, 7–12; (d) R. Ballerstadt, C. Evans, R. McNichols and A. Gowda, *Biosens. Bioelectron.*, 2006, **22**, 275–284; (e) L. Yu, M. Huang, P. G. Wang and X. Zeng, *Anal. Chem.*, 2007, **79**, 8979–8986; (f) C. Guo, P. Boullanger, L. Jiang and T. Liu, *Biosens. Bioelectron.*, 2007, **22**, 1830–1834.
 - 14 D. Pallarola and F. Battaglini, *Anal. Biochem.*, 2008, **381**, 53–58.
 - 15 E. M. Kober, J. V. Caspar, B. P. Sullivan and T. J. Meyer, *Inorg. Chem.*, 1988, **27**, 4587–4598.
 - 16 H. Haas and H. Möhwald, *Thin Solid Films*, 1989, **180**, 101–110.
 - 17 E. Stenberg, B. Persson, H. Roos and C. Urbaniczky, *J. Colloid Interface Sci.*, 1991, **143**, 513–526.
 - 18 F. Yu, PhD Thesis, Johannes Gutenberg-Universität, Mainz, Germany, 2004.
 - 19 (a) A. Monzo, G. K. Bonn and A. Guttman, *TrAC, Trends Anal. Chem.*, 2007, **26**, 423–432; (b) B. M. Brena and F. Batista-Viera, in *Methods in Biotechnology: Immobilization of Enzymes and Cells*, ed. J. M. Guisán, Humana Press Inc., Totowa, 2006, ch. 2, pp. 15–30.
 - 20 (a) C. Barnes, C. D'Silva, J. P. Jones and T. J. Lewis, *Sens. Actuators B*, 1991, **3**, 295–304; (b) S. Liu, K. Wang, D. Du, Y. Sun and L. He, *Biomacromolecules*, 2007, **8**, 2142–2148; (c) L. Tan, Q. Xie and S. Yao, *Bioelectrochemistry*, 2007, **70**, 348–355.
 - 21 (a) H. Bittinger and H. P. Schnebli, *Concanavalin A as a Tool*, John Wiley & Sons, London, 1976; (b) M. C. Chervenak and E. J. Toone, *Biochemistry*, 1995, **34**, 5116–5120.
 - 22 N. Horan, L. Yan, H. Isobe, G. M. Whitesides and D. Kahne, *Proc. Natl. Acad. Sci. U. S. A.*, 1999, **96**, 11782–11786.
 - 23 E. A. Smith, W. D. Thomas, L. L. Kiessling and R. M. Corn, *J. Am. Chem. Soc.*, 2003, **125**, 6140–6148.
 - 24 Y. Ebara and Y. Okahata, *J. Am. Chem. Soc.*, 1994, **116**, 11209–11212.
 - 25 (a) T. Fukuda, S. Onogi and Y. Miura, *Thin Solid Films*, 2009, **518**, 880–888; (b) Y. Sato, T. Murakami, K. Yoshioka and O. Niwa, *Anal. Bioanal. Chem.*, 2008, **391**, 2527–2532; (c) Q. Yang, M.-X. Hu, Z.-W. Dai, J. Tian and Z.-K. Xu, *Langmuir*, 2006, **22**, 9345–9349.
 - 26 (a) A. Yoshizumi, N. Kanayama, Y. Maehara, M. Ide and H. Kitano, *Langmuir*, 1999, **15**, 482–488; (b) D. J. Revell, J. R. Knight, D. J. Blyth, A. H. Haines and D. A. Russell, *Langmuir*, 1998, **14**, 4517–4524; (c) Y. Miura, T. Yamauchi, H. Sato and H. Fukuda, *Thin Solid Films*, 2008, **516**, 2443–2449; (d) Y. Zhang, S. Luo, Y. Tang, L. Yu, K.-Y. Hou, J.-P. Cheng, X. Zeng and P. G. Wang, *Anal. Chem.*, 2006, **78**, 2001–2008.
 - 27 (a) C. Guo, P. Boullanger, L. Jiang and T. Liu, *Colloids Surf., B*, 2008, **62**, 146–150; (b) K. Larsen, M. B. Thygesen, F. Guillaumie, W. G. T. Willats and K. J. Jensen, *Carbohydr. Res.*, 2006, **341**, 1209–1234; (c) M. Huang, Z. Shen, Y. Zhang, X. Zeng and P. G. Wang, *Bioorg. Med. Chem. Lett.*, 2007, **17**, 5379–5383; (d) M. Niwa, T. Mori, E. Nishio, H. Nishimura and N. Higashi, *J. Chem. Soc., Chem. Commun.*, 1992, 547–549; (e) M. Kadalbajoo, J. Park, A. Opdahl, H. Suda, C. A. Kitchens, J. C. Garino, J. D. Batteas, M. J. Tarlov and P. DeShong, *Langmuir*, 2007, **23**, 700–707.
 - 28 I. Willner, S. Rubin and Y. Cohen, *J. Am. Chem. Soc.*, 1993, **115**, 4937–4938.
 - 29 G. Sauerbrey, *Z. Phys.*, 1959, **155**, 206–222.
 - 30 M. Rodahl, P. Dahquist, F. Höök and B. Kasemo, in *Biomolecular Sensors*, ed. E. Gizeli and C. R. Lowe, Taylor & Francis, London, 2002, ch. 12, pp. 304–316.
 - 31 E. D. Kaufman, J. Belyea, M. C. Johnson, Z. M. Nicholson, J. L. Ricks, P. K. Shah, M. Bayless, T. Pettersson, Z. Feldoto, E. Blomberg, P. Claesson and S. Franzen, *Langmuir*, 2007, **23**, 6053–6062.
 - 32 O. Azzaroni, M. Álvarez, A. I. Abou-Kandil, B. Yameen and W. Knoll, *Adv. Funct. Mater.*, 2008, **18**, 3487–3496.
 - 33 S. M. Notley, M. Eriksson and L. Wagberg, *J. Colloid Interface Sci.*, 2005, **292**, 29–37.
 - 34 J.-i. Anzai and Y. Kobayashi, *Langmuir*, 2000, **16**, 2851–2856.
 - 35 (a) F. Höök, M. Rodahl, P. Brzezinski and B. Kasemo, *J. Colloid Interface Sci.*, 1998, **208**, 63–67; (b) F. Höök, M. Rodahl, P. Brzezinski and B. Kasemo, *Langmuir*, 1998, **14**, 729–734.
 - 36 (a) C. Larsson and M. Rodahl, *Anal. Chem.*, 2003, **75**, 5080–5087; (b) F. Höök, A. Ray, B. Nordén and B. Kasemo, *Langmuir*, 2001, **17**, 8305–8312.
 - 37 W. Knoll, *Annu. Rev. Phys. Chem.*, 1998, **49**, 569.
 - 38 E. Reimhult, C. Larsson, B. Kasemo and F. Höök, *Anal. Chem.*, 2004, **76**, 7211–7220.
 - 39 O. Azzaroni, M. Mir and W. Knoll, *J. Phys. Chem. B*, 2007, **111**, 13499–13503.
 - 40 (a) T. Ikeda, *Chem. Rec.*, 2004, **4**, 192–203; (b) W. Katz, A. N. Shipway and I. Willner, in *Bioelectrochemistry*, ed. G. S. Wilson, Wiley-VCH, Weinheim, 2002, ch. 17, pp. 559–626.
 - 41 C. Demaille, J. Moiroux, J.-M. Savéant and C. Bourdillon, in *Protein Architecture: Interfacing Molecular Assemblies and Immobilization Biotechnology*, ed. Y. Lvov and H. Möhwald, Marcel Dekker, New York, 2000, ch. 12, pp. 311–335.
 - 42 J. M. Savéant, *Elements of Molecular and Biomolecular Electrochemistry: An Electrochemical Approach to Electron Transfer Chemistry*, Wiley-Interscience, Hoboken, 2006, ch. 5, pp. 298–347.
 - 43 (a) C. Bourdillon, C. Demaille, J. Moiroux and J.-M. Savéant, *Acc. Chem. Res.*, 1996, **29**, 529–535; (b) C. Bourdillon, C. Demaille, J. Moiroux and J.-M. Savéant, *J. Am. Chem. Soc.*, 1994, **116**, 10328–10329.
 - 44 (a) C. Bourdillon, C. Demaille, J. Moiroux and J.-M. Savéant, *J. Am. Chem. Soc.*, 1995, **117**, 11499–11506; (b) A. Anicet, A. Anne, J. Moiroux and J.-M. Savéant, *J. Am. Chem. Soc.*, 1998, **120**, 7115–7116.
 - 45 M. Campàs i Homs, *PhD Thesis*, Universitat Rovira i Virgili, Tarragona, Spain, ch. 5, 2002, pp. 113–137. <http://www.tdx.cat/TDX-1104102-091806>.
 - 46 C. Danilowicz, E. Cortón and F. Battaglini, *J. Electroanal. Chem.*, 1998, **445**, 89–94.
 - 47 V. Flexer, E. S. Forzani, E. J. Calvo, S. J. Ludueña and L. I. Pietrasanta, *Anal. Chem.*, 2006, **78**, 399–407.
 - 48 V. Flexer, M. V. Ielmini, E. J. Calvo and P. N. Bartlett, *Bioelectrochemistry*, 2008, **74**, 201–209.
 - 49 C. Bourdillon, C. Demaille, J. Moiroux and J.-M. Savéant, *J. Am. Chem. Soc.*, 1993, **115**, 12264–12269.
 - 50 (a) X.-H. Dai, C.-M. Dong and D. Yan, *J. Phys. Chem. B*, 2008, **112**, 3644–3652; (b) D. Kitamoto, S. Ghosh, G. Ourisson and Y. Nakatani, *Chem. Commun.*, 2000, 861–862; (c) G. Chen, L. Tao, G. Mantovani, J. Geng, D. Nystrom and D. M. Haddleton, *Macromolecules*, 2007, **40**, 7513–7520; (d) J. Geng, G. Mantovani, L. Tao, J. Nicolas, G. Chen, R. Wallis, D. A. Mitchell, B. R. G. Johnson, S. D. Evans and D. M. Haddleton, *J. Am. Chem. Soc.*, 2007, **129**, 15156–15163; (e) J. M. Belitsky, A. Nelson, J. D. Hernandez, L. G. Baum and J. F. Stoddart, *Chem. Biol.*, 2007, **14**, 1140–1151; (f) J. Park, L. H. Rader, G. B. Thomas, E. J. Danoff, D. S. English and P. DeShong, *Soft Matter*, 2008, **4**, 1916–1921; (g) J. F. Rusling, E. G. Hvastkovs, D. O. Hull and J. B. Schenkman, *Chem. Commun.*, 2008, 141–154; (h) D. Sarauli, J. Tanne, D. Schäfer, I. W. Schubart and F. Lisdat, *Electrochem. Commun.*, 2009, **11**, 2288–2291; (i) L. M. Moretto, P. Bertocello, F. Vezzà and P. Ugo, *Bioelectrochemistry*, 2005, **66**, 29–34; (j) M. Fang, P. S. Grant, M. J. McShane, G. B. Sukhorukov, V. O. Golub and Y. M. Lvov, *Langmuir*, 2002, **18**, 6338–6344; (k) Y. Lvov, K. Ariga, I. Ichinose and T. Kunitake, *J. Am. Chem. Soc.*, 1995, **117**, 6117–6123; (l) X. Yan, H.-F. Ji and Y. Lvov, *Chem. Phys. Lett.*, 2004, **396**, 34–37.
 - 51 (a) S. Takeoka, K. Sou, T. Ohgushi and E. Tsuchida, *Supramol. Sci.*, 1998, **5**, 159–162; (b) T. Cassier, K. Lowack and G. Decher, *Supramol. Sci.*, 1998, **5**, 309–315; (c) Y. Lvov, K. Ariga, I. Ichinose

- and T. Kunitake, *J. Chem. Soc., Chem. Commun.*, 1995, 2313–2315; (d) Y. Lvov, K. Ariga, I. Ichinise and T. Kunitake, *Thin Solid Films*, 1996, **284–285**, 797–801.
- 52 (a) J.-i. Anzai, Y. Kobayashi, N. Nakamura and T. Hoshi, *Sens. Actuators, B*, 2000, **65**, 94–96; (b) Y. Kobayashi, T. Hoshi and J.-i. Anzai, *Chem. Pharm. Bull.*, 2001, **49**, 755–757.
- 53 (a) B. Ivarsson and M. Malmqvist, in *Biomolecular Sensors*, ed. E. Gizeli and C.R. Lowe, Taylor & Francis, London, 2002, ch. 9, pp. 241–268; (b) P. B. Garland, *Q. Rev. Biophys.*, 1996, **29**, 91–117.
- 54 (a) O. Azzaroni, M. Mir, M. Álvarez, B. Yameen and W. Knoll, *J. Phys. Chem. C*, 2008, **112**, 15850–15859; (b) O. Azzaroni, M. Mir, M. Álvarez, L. Tiefenauer and W. Knoll, *Langmuir*, 2008, **24**, 2878–2883; (c) M. Mir, M. Álvarez, O. Azzaroni, L. Tiefenauer and W. Knoll, *Anal. Chem.*, 2008, **80**, 6554–6569.
- 55 (a) L.-C. You, F.-Z. Lu, Z.-C. Li, W. Zhang and F.-M. Li, *Macromolecules*, 2003, **36**, 1–4; (b) E. S. Gil and S. M. Hudson, *Prog. Polym. Sci.*, 2004, **29**, 1173–1222; (c) T. Miyata, A. Jikihara, K. Nakamae and A. S. Hoffman, *Macromol. Chem. Phys.*, 1996, **197**, 1135–1146.
- 56 (a) R. Ballerstadt and J. S. Schultz, *Sens. Actuators, B*, 1998, **46**, 50–55; (b) K. Tagawa, N. Sendai, K. Ohno, T. Kawaguchi and H. Kitano, *Bioconjugate Chem.*, 1999, **10**, 354–360; (c) K. Sato, Y. Imoto, J. Sugama, S. Seki, H. Inoue, T. Odagiri, T. Hoshi and J.-i. Anzai, *Langmuir*, 2005, **21**, 797–799.
- 57 J. M. Abad, M. Vélez, C. Santamaría, G. M. Guisán, P. R. Matheus, L. Vázquez, I. Gazaryan, L. Gorton, T. Gibson and V. M. Fernández, *J. Am. Chem. Soc.*, 2002, **124**, 12845–12853.
- 58 (a) K. Sato and J.-i. Anzai, *Anal. Bioanal. Chem.*, 2006, **384**, 1297–1301; (b) K. Sato, Y. Imoto, J. Sugama, S. Seki, H. Inoue, T. Odagiri and J.-i. Anzai, *Anal. Sci.*, 2004, **20**, 1247–1248; (c) K. Sato, D. Kodama and J.-i. Anzai, *Anal. Bioanal. Chem.*, 2006, **386**, 1899–1904.
- 59 (a) H. Lis and N. Sharon, *Chem. Rev.*, 1998, **98**, 637–674; (b) N. Sharon, *J. Biol. Chem.*, 2006, **282**, 2753–2764; (c) N. Sharon and H. Lis, *Glycobiology*, 2004, **14**, 53R–62R.
- 60 W. M. B. Yunus and A. B. Rahman, *Appl. Opt.*, 1988, **27**, 3341–3343.
- 61 (a) M. I. Khan, D. K. Mandal and C. F. Brewer, *Carbohydr. Res.*, 1991, **213**, 69–77; (b) E. E. Snyder and R. Fall, *Biochem. Educ.*, 1990, **18**, 147–148; (c) K.-J. Schott, V. Neuhoff, B. Nessel, U. Pötter and J. Schröter, *Electrophoresis*, 1984, **5**, 77–83;
- (d) V. L. Arvanov, M. C. Tsai, R. J. Walker and S. N. Ayrapietian, *Brain Res.*, 1993, **615**, 252–258; (e) J. H. M. Davina, A. M. Stadhouders, U. J. G. M. van Haelst, R. de Graaf and P. Kenemans, *Cancer Research*, 1986, **46**, 1539–1543; (f) S. S. Lin and I. B. Levitan, *Trends Neurosci.*, 1991, **14**, 273–277; (g) K. I. Hardman, R. C. Agarwal and M. J. Freiser, *J. Mol. Biol.*, 1982, **157**, 69–86; (h) P. Sheterline and C. R. Hopkins, *J. Cell Biol.*, 1981, **90**, 743–754.
- 62 (a) M. Wilczewski, A. Van der Heyden, O. Renaudet, P. Dumy, L. Coche-Guerente and P. Labbé, *Org. Biomol. Chem.*, 2008, **6**, 1114–1122; (b) M. L. Wolfenden and M. J. Cloninger, *Bioconjugate Chem.*, 2006, **17**, 958–966; (c) L. L. Kiessling, J. E. Gestwicki and L. E. Strong, *Curr. Opin. Chem. Biol.*, 2000, **4**, 696–703; (d) H. M. Branderhorst, R. Ruijtenbeek, R. M. J. Liskamp and R. J. Pieters, *ChemBioChem*, 2008, **9**, 1836–1844; (e) E. K. Woller, E. D. Walter, J. R. Morgan, D. J. Singel and M. J. Cloninger, *J. Am. Chem. Soc.*, 2003, **125**, 8820–8826; (f) T. K. Dam, R. Roy, S. K. Das, S. Oscarson and C. F. Brewer, *J. Biol. Chem.*, 2000, **275**, 14223–14230; (g) M. Kanai, K. H. Mortell and L. L. Kiessling, *J. Am. Chem. Soc.*, 1997, **119**, 9931–9932; (h) E. K. Woller and M. J. Cloninger, *Biomacromolecules*, 2001, **2**, 1052–1054; (i) T. K. Dam and C. F. Brewer, *Biochemistry*, 2008, **47**, 8470–8476; (j) D. A. Mann, M. Kanai, D. J. Maly and L. L. Kiessling, *J. Am. Chem. Soc.*, 1998, **120**, 10575–10582; (k) L. L. Kiessling, J. E. Gestwicki and L. E. Strong, *Angew. Chem., Int. Ed.*, 2006, **45**, 2348–2368.
- 63 C. R. Bertozzi and L. L. Kiessling, *Science*, 2001, **291**, 2357–2363.
- 64 M. N. Liang, S. P. Smith, S. J. Metallo, I. S. Choi, M. Prentiss and G. M. Whitesides, *Proc. Natl. Acad. Sci. U. S. A.*, 2000, **97**, 13092–13096.
- 65 J. C. Jones, J. C. Pinkner, R. Roth, J. Heuser, A. V. Nicholes, S. N. Abraham and S. J. Hultgren, *Proc. Natl. Acad. Sci. U. S. A.*, 1995, **92**, 2081–2085.
- 66 K. H. Mortell, R. V. Weatherman and L. L. Kiessling, *J. Am. Chem. Soc.*, 1996, **118**, 2297.
- 67 G. Decher, in *Multilayer Thin Films: Sequential Assembly of Nanocomposite Materials*, ed. G. Decher and J. B. Schlenoff, Wiley-VCH, Weinheim, 2002, ch. 1, pp. 1–46.
- 68 R. Liang, L. Yan, J. Loebach, M. Ge, Y. Uozumi, K. Sekanina, N. Horan, J. Glidersleeve, C. Thompson, A. Smith, K. Biswas, W. C. Still and D. Kahne, *Science*, 1996, **274**, 1520–1522.